



Molecular dynamics simulations of microstructure and mixing dynamics of cryoprotective solvents in water and in the presence of a lipid membrane

Alexander Kyrychenko ^{a,*}, Tatyana S. Dyubko ^b

^a Institute for Chemistry, V. N. Karazin Kharkov National University, 4 Svobody Sq., 61077, Kharkov, Ukraine

^b Institute for Problems of Cryobiology and Cryomedicine of the National Academy of Sciences of Ukraine, 23 Pereyaslavskaya Str., Kharkov, 61015, Ukraine

ARTICLE INFO

Article history:

Received 11 February 2008

Received in revised form 7 April 2008

Accepted 8 April 2008

Available online 18 April 2008

Keywords:

Molecular dynamics simulation

Cryoprotective solvent

Self-association

Hydrogen-bonding

Lipid membrane

ABSTRACT

Molecular dynamics (MD) simulation is used to investigate the solubility behavior of cryoprotective (CP) solvents, such as DMSO, ethylene glycol (EG) and glycerol (GL), in pure water and in the presence of a lipid membrane. The MD study is focused on an equilibration timescale required for mixing large CP aggregates with aqueous and aqueous/lipid environments. The MD analysis demonstrates that DMSO mixes rapidly with water, so that all solute molecules are uniformly distributed in the equilibrium aqueous solution. Our investigation of the microstructure of binary EG/water and GL/water systems reveals that, despite the miscibility of both CP solvents with water, they are not ideally mixed in aqueous solutions at the molecular level. The MD simulations show that the mixing dynamics of the large CP cluster and surrounding water is found to be strongly dependent on nature of hydrophilic and hydrophobic interactions acting between cryoprotectant molecules. In particular, a spatial hydrogen-bond network formed between CP molecules plays an important role in the mixing dynamics between CP agents and water. A further analysis on the mixing behavior of the CP solvents with pure water and with aqueous solutions at a lipid membrane interface shows that, due to strong binding of the CP molecules to membrane surface, the equilibration process in the lipid environment becomes very slow, at least of the order of microseconds. The MD results are discussed in the context of the better understanding on the composition of the aqueous mixtures of the EG and GL solvents. Knowledge of the microstructure and the dynamics of these systems helps to develop better cryopreservation protocols and to propose more optimal cooling/warming regimes for cellular cryosolutions.

© 2008 Elsevier B.V. All rights reserved.

1. Introduction and motivation

Aqueous mixtures of organic solvents such as glycols, sugars and DMSO are widely used as a cryoprotective (CP) agent to preserve biological systems during freezing. A cryoprotection mechanism is based on an idea that CP agents suppress crystallization in cell water by inducing the formation of a glassy state [1]. It is commonly believed that cryoprotective solvents alter certain colligative properties of water solution. At a molecular level, it is expected that in the presence of CP molecules the H-bonded network structure of bulk water is broken, so that this perturbation results in slowing down of the water dynamics. The microstructure of cryoprotective solutions, which consist of CP solvents enabling efficient H-bonding with water, such as glycols and higher alcohols is, therefore, viewed to be very rich and complex. It is well established that, when alcohol content is varied, the thermodynamic functions and spectroscopic properties of binary alcohol/water solutions demonstrate unexpected maxima and inflection points. The composition-property dependencies also differ significantly from the behavior that might be expected for an ideal

mixture of the same pure liquids. The nonideal thermodynamic and transport properties of aqueous solutions of lower alcohols are often interpreted in terms of either local structure changes in the mixture [2] or molecular aggregation and self-association of alcohol molecules [3–9]. Despite the apparent miscibility of both components in all proportions, modern diffraction experiments have shown the existence of clathrate structures and alcohol clustering [10–12]. These findings lead, therefore, to a new insight into the mixing behavior and the heterogeneous structure of aqueous solution of organic solvents containing both hydrophobic and hydrophilic groups. In addition, computer modeling is also found to be a very promising tool to assist explanation of the microstructure of binary mixtures. The structure of aqueous solutions containing CP solvents is widely studied by applying of molecular dynamics (MD) simulation methods [13–17]. Analysis of the solution microstructure has shown that, depending on concentrations, some CP solvents are characterized by inhomogeneous dispersion in solution due to their self-association and aggregation [13,14]. It is also interesting to note that the solvent clustering in aqueous solution is found to be strongly sensitive to temperature changes. Lowering the temperature has been shown to enhance the greater molecular heterogeneity in binary mixtures, so that structural parameters, sizes and distributions of labile solvent

* Corresponding author. Tel.: +380 57 707 5335.

E-mail address: alexander.v.kyrychenko@univer.kharkov.ua (A. Kyrychenko).

aggregates are changed [18,19]. These temperature changes are often accompanied by an increase of solution viscosity. As a result, diffusion processes in these low-temperature mixtures are slowed down dramatically. Such a temperature behavior seems to be particularly important for low-temperature cryosolutions. The appearance of large microheterogeneity gradients may depend on a cooling rate. Therefore, at these conditions the formation of some non-equilibrium solvent aggregates is expected. It has recently been demonstrated for solutions containing glycerol as a CP agent that the response of cells such as spermatozoa and red blood cells is found to be particularly sensitive for a cooling regime [20]. It has been concluded that, in the case of the rapid cooling, the composition and the ultrastructure of the freeze matrix around cells deviate significantly from the properties, which are found in the slowly cooled equilibrium cryosolution. These findings point out that the “effective” concentration of CP molecules in cellular solution might, in principle, be dependent on different thermal treatments of the system. The concentration of the “active” CP molecules may also be influenced by the method of their introduction into solution, as either a single aliquot or in a stepwise manner. Since bulk structural properties of liquids depend on their microheterogeneous structure, it is important to understand the influence of this microheterogeneity on the efficiency of interactions of CP agents with a biomolecule. However, at present there still is no generally accepted understanding of what is the most effective way of addition of cryoprotector into biorelevant systems, as either rapid one-step or slow step-by-step addition.

A series of experimental data has suggested that the fractionated dilution of cryoprotector is more beneficial than the single-step direct dilution [21–23]. The better tolerance for cryoconservation of leucocytes was obtained during slow addition of DMSO to cellular solution at 22 °C [22]. Corneas, immersed directly into 3 M DMSO, were irreparably damaged irrespective of the method of dilution [23]. At the same time, sequential addition of 1, 2 and 3 M DMSO followed by the fractionated dilution was tolerated by endothelium and minor alterations to the structural integrity of the endothelial layer were rapidly repaired. However, the authors of this study have only discussed and analyzed the osmotic nature of these observations. Also, the correlation between the positive effect of the stepwise addition of the cryoprotector and the structural heterogeneity of aqueous cryosolution has not been analyzed in details, so that the obtained results are mainly explained in terms of minimization of the osmotic stress to endothelium during the fractionated dilution. It should also be noted that, on the other hand, no reliable difference was observed in the case of the quality of canine semen, which has been submitted to either single or fractionated glycerol addition during the freezing process [24]. Therefore, additional studies are needed to explain, on a molecular level, reasons for observed features appearing due to some differences in cryopreservation protocols. In addition, many experimental results have indicated that CP agents reveal cytotoxicity with respect to biomembranes and intracellular structures. This cytotoxicity is often observed not directly during freezing, but rather during the equilibration time prior to freezing and also during post-thawing periods [25–28]. Moreover, the importance of concentration of CP agents and the incubation temperature has also been emphasized [29]. In spite of many experimental studies, possible mechanisms of the cytotoxic action of CP agents on biomembranes are still not evident so far.

In this study, we are interested in investigating the dynamics of the mixing of various CP agents (DMSO, ethylene glycol, and glycerol) with water. Our study is focused on characterizing the slow kinetics of destruction of large CP aggregates in aqueous solutions. The CP–water mixing behavior in binary solution will be analyzed by applying the MD methodology. We are also interested in determining what kind of molecular properties of CP solvents is responsible for their anomalous cryoprotective actions on biological membranes. Therefore, the influence of the lipid membrane on the microstructure of cryopro-

tectant solutions is also studied. The MD method is widely employed in studying, with the atomic resolution, interactions and the partitioning behavior of organic solvents with phospholipid bilayers and biomembranes [30–36]. Knowledge and a deeper understanding of the cryoprotection mechanism would help us with the design of better solvent mixtures to improve the cryopreservation properties and cooling/warming procedures.

2. System setup and MD simulation details

The MD simulations were carried out using the GROMACS set of programs, version 3.0 [37]. The cryoprotective solvents were modeled using force fields available for DMSO [38], ethylene glycol (EG) [39–41] and glycerol (GL) [42–44]. The corresponding parameterization was adopted for the GROMACS force field. In the case of EG and GL, the aliphatic CH and CH₂ fragments were represented by the united atom approximation. The mixing behavior of CP solvents and water was studied by analyzing the distribution of CP molecules in aqueous solution. The microstructure of the binary solutions was also examined by monitoring of time evolution of intermolecular hydrogen-bonds in the CP/water systems. To determine if an H-bond exists between all possible H-bond donor (D) and acceptor (A) atoms, geometrical criteria were used. These criteria were based on the H-bond distance and angle cut-offs, $R_{DA} \leq 0.35$ nm and $\theta_{DHA} = 180^\circ \pm 30^\circ$, respectively.

A biomembrane was modeled by a lipid bilayer consisting of 88 dipalmitoylphosphatidylcholine (DPPC) lipids (44 per leaflet). Similarly to the CP molecules, all carbon atoms of methylene and methyl groups of the lipids with non-polar hydrogens are also treated as united atoms. An initial configuration of a DPPC bilayer was taken from ref [45]. The bilayer force field is based on the modified OPLS parameterizations [45]. The Simple Point Charge (SPC) model was applied for the water modeling [46]. The simulation temperature was chosen to be equal to 323 K. The whole system was first equilibrated for 200 ps at the constant number of particles, constant pressure, $P=1$ atm, and constant temperature, $T=323$ K (NPT ensemble). Three-dimensional periodic boundary conditions were applied for the MD simulation box. The z-axis of the box was directed along the bilayer normal. The pressure was controlled semi-isotropically, so that the x- and y dimensions of the simulation box were allowed to fluctuate independently from each other keeping the total pressure constant. Thus, the membrane area and thickness were free to adjust under the constant pressure condition. The reference temperature and pressure were kept constant using the weak coupling scheme [47] with a coupling constant of $\tau_p=0.1$ ps for temperature coupling and $\tau_\pi=1.0$ ps for pressure coupling. A twin-range cutoff scheme was employed in the simulations of electrostatic interactions using the particle mesh Ewald (PME) approach [48]. Short-range electrostatic interactions were calculated for every time step within sphere of 1.0 nm radius. Long-range interactions were evaluated within the cutoff 1.8 nm every 10 fs. The cutoff distance of Lennard–Jones interactions was also equal to 1.8 nm. The evaluated pair interaction list was kept constant until the next update. The integration time step was 2 fs. All bond lengths in DPPC and CP molecules were kept constant using the LINCS routine [49]. The similar MD setup has been demonstrated to be the optimal for the simulations of the equilibrium properties of the DPPC bilayer [50].

3. Results and discussion

We have organized the article as follows. We first present the characteristics of the simulated systems. We describe the MD simulation results of the mixing process in which the two preformed phases, consisting of CP solvent and water, are allowed to mix freely with each other. Distributions of the CP molecules in the binary systems are analyzed as a function of the mixing time. In the next section, the mixing

dynamics is studied for the ternary CP/membrane/water systems, in which a lipid membrane is represented by a DPPC bilayer. The CP solvents, which are initially placed as a thin layer at a membrane interface, are considered in terms of their solubility dynamics in aqueous solution. The comparison of the mixing behavior of the three different CP solvents with water as a function of the mixing time and the influence of the lipid membrane on the CP–water mixing dynamics are discussed.

3.1. Characteristics of simulated systems

Three CP solvents, DMSO, ethylene glycol (EG), and glycerol (GL) are considered. Initial configurations of the CP/water systems were prepared as follows. Each bulk CP solvent was originally equilibrated in a cubic box by running the NPT-simulations with the 3D-periodic boundary conditions. The equilibration time was equal to 2–4 ns. After the equilibration period, the size of the MD box was increased along the *z*-axis, so that the CP solvent phase was kept in the middle of the simulation cell. The free volume of the MD cell expanded along the *z*-axis was filled by water molecules. Thus, the new water phase surrounds the CP solvent from its both sides, Fig. 1(top). A set of short MD equilibration runs was performed, during which only one of either CP or water components was allowed to relax. At the same time, all molecules belonging to the second phase were kept at their fixed positions. In this way, in the initial MD system the “preformed” bulk phase of the CP solvent was kept to be separated from the water phase. As an example, the MD cell of the initial EG/water system is shown in Fig. 1(top). The composition and characteristics of the studied binary systems consisting of the CP solvents and water are given in Table 1.

The influence of the biomembrane interface on the mixing dynamics of the CP agents with water is studied for the same set of three CP solvents in the presence of the DPPC lipid bilayer. The initial ternary systems containing CP, membrane and water components were prepared in the fashion which is similar to that of the CP/water binary systems. The DPPC membrane was placed in the middle of a rectangular MD simulation cell. A thin layer of the CP solvent is added at the membrane interface on the top and bottom sides of the bilayer.

Table 1
Characteristics of the binary and ternary systems

System	CP	Water	DPPC	Box size (Å)	Time (ns)
DMSO/water	272	4033	–	42.4×42.4×98.3	5
EG/water	498	4350	–	44.5×44.5×91.4	25
GL/water	310	4205	–	40.9×40.9×99.0	30
DMSO/DPPC/water	272	4033	88	52.2×52.2×108.2	7
EG/DPPC/water	498	5370	88	52.2×52.2×120.1	15
GL/DPPC/water	310	4706	88	52.2×52.2×105.0	20

Finally, the free volume of the simulation cell was filled by water molecules. The initial EG/membrane/water system is schematically shown in Fig. 1(bottom). To be able to compare the behavior of the CP/water binary mixtures to the corresponding CP/membrane/water ternary systems, the same number of the CP molecules was, therefore, chosen in the both cases. To avoid high energy contacts and thermal instability, the initial ternary systems were also pre-equilibrated by a series of energy minimization and short MD runs, during which only one of the components is allowed to relax, whereas, the rest of the system is kept at rigid positions. The compositions of the studied ternary systems are also shown in Table 1.

3.2. MD simulations of CP/water binary systems

We performed a set of MD simulations in order to elucidate the mixing behavior of a series of CP solvents with aqueous solution. The simulations are based on the passive mixing between the CP solvent and water phases. The mixing is driven by thermal diffusion. The “preformed” bulk phase of the CP solvent was allowed to dissolve freely in water during the nanosecond-scale MD simulations carried out at the NPT conditions. The solubility of the CP solvents as a function of a mixing time (t_m) was studied. The structure of the binary solutions was monitored by examining of its macro- and microscopic properties at different t_m .

One of macroscopic parameters describing the mixing behavior is a mass density distribution of a component in a binary system. Such a density distribution for each of the two, CP and water, components was calculated along the long *z*-axis of the MD cell as a function of t_m . Due to symmetry reasons, the component densities are plotted with respect to the center of the *z*-axis placed in the middle of the MD cell, Fig. 1(top). Fig. 2 shows the density profiles for the studied CP/water binary systems. The densities are calculated at different time intervals starting from the beginning of the mixing process. The two well-defined separate phases may be seen in all the initial systems at the beginning of the MD simulation, at $t_m=0$ ns. The averaged water density profile is plotted for the initial system only, while the mass density distributions of the CP components are additionally shown for intermediate t_m .

The mass density distributions of the water and DMSO phases corresponding to $t_m=0$ ns are shown by solid lines in Fig. 2(a). The average mass densities estimated for the pure DMSO and water phases agree with experimental values. As can be seen in Fig. 2(a), the well-defined separation between water and DMSO observed at $t_m=0$ ns starts to disappear since approximately 0.8 ns from the beginning of the phase mixing. As mentioned above, in the case of the intermediate time intervals, only the DMSO density distributions are plotted for clarity. An arrow shows the time evolution of the DMSO mass density during the mixing. The MD results demonstrate that the DMSO density becomes almost equally distributed along the MD box after the mixing period of approximately 3–5 ns, Fig. 2(a). At the same time, the analysis of the microstructure of the binary mixture on the molecular level indicates that all DMSO molecules are homogeneously dispersed in aqueous solution. Thus, the study of the mixing dynamics in the DMSO/water system shows that the DMSO phase is completely solubilized in water during approximately 5 ns.

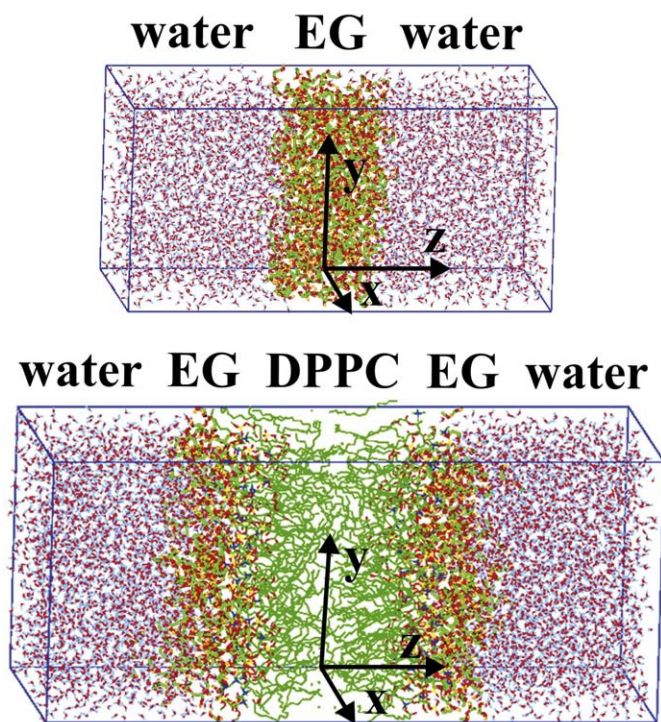


Fig. 1. Schematic representation of the EG/water (top) and the EG/DPPC-membrane/water (bottom) systems.

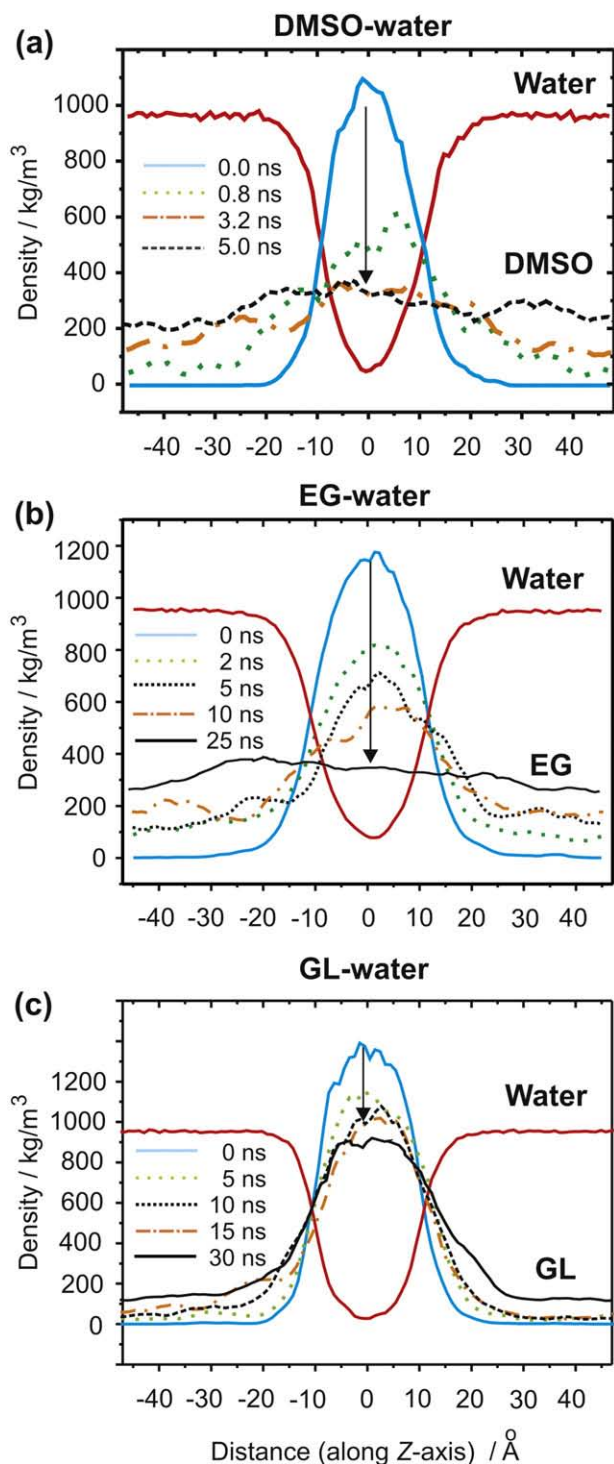


Fig. 2. Mass density profiles of the two components in the CP/water systems are shown as a function of the mixing time (in nanoseconds). The density curves for DMSO–water (a), EG–water (b) and GL–water (c) are plotted with respect to the center of the z-axis of the MD cell. The water density is shown for $t_m=0$ ns only.

Knowledge of hydrogen-bonding occurring between DMSO and water molecules is important for understanding how this CP solvent acts as a colligative solute [13–15]. Therefore, the mixing dynamics of bulk DMSO with aqueous solution is also studied on a molecular level by applying a hydrogen-bonding analysis. The total number of intermolecular hydrogen-bonds, which are formed between all DMSO and water molecules, is calculated during the MD simulation of the mixing process as a function of time. The hydrogen-bonds are calculated with a time step of 20 fs. Fig. 3 shows the total number of

the hydrogen-bonds in the DMSO/water binary system as a function of t_m . One DMSO molecule may form two intermolecular hydrogen-bonds with two water molecules. The structure of such a hydrogen-bonded complex is schematically shown in Fig. 3. The total number of 544 H-bonds may therefore be expected between all 272 DMSO molecules and the surrounding water. Such a limit of the hydrogen-bond number is plotted as a dotted line in Fig. 3. As seen from Fig. 3, the total number of the DMSO–water H-bonds increases rapidly from 150 at $t_m=0$ ns to a nearly constant value of about 540 at $t_m=3$ ns. Starting since approximately $t_m=3$ ns, the total number of hydrogen-bonds reaches a well-defined plateau asymptotically. It corresponds to the theoretical limit of hydrogen-bonding between DMSO and water molecules for this system. Thus, in the equilibrium binary solution each DMSO molecule forms the two hydrogen-bonds with the surrounding bulk water.

The time evolutions of the mass densities of the CP and water components are shown for the EG/water and GL/water binary systems in Fig. 2(b) and (c), respectively. As can be seen from Fig. 2(b), the mass density peak of the EG phase is observed at the center of the z-axis at $t_m=0$ ns. During the phase mixing, the EG density is slowly distributed within the MD cell; however, it should also be noted that the separate EG phase may still be observed in the system even after the mixing period of approximately 5 ns.

Fig. 4 shows snapshots of MD boxes calculated at different t_m . As can be seen, the interface between the two phases, which is defined in Fig. 2(b) as the intersection between the EG and water density curves at $t_m=0$ ns, becomes irregular at $t_m=2$ ns due to the interphase mixing. The phase separation between EG and water starts to disappear only at $t_m=10$ –15 ns. In Fig. 4(a), the distribution of the EG molecules in the EG/water binary system is shown for the intermediate mixing time intervals. In addition, the study of the microstructure of the binary solution as a function of t_m demonstrates that the initial EG bulk-like phase is being gradually depleted into various aggregates of smaller sizes. These aggregates are not static and they are found to be in equilibrium with other labile aggregates of different sizes. As a result, the distribution of the EG molecules demonstrates the strong heterogeneity in the system during first 10 ns of the mixing, Fig. 4(a). The two liquids are found to be mixed almost completely only after approximately 25 ns.

Fig. 4(b) shows the distribution of the GL molecules in the GL/water system at different t_m . The water molecules are not shown for

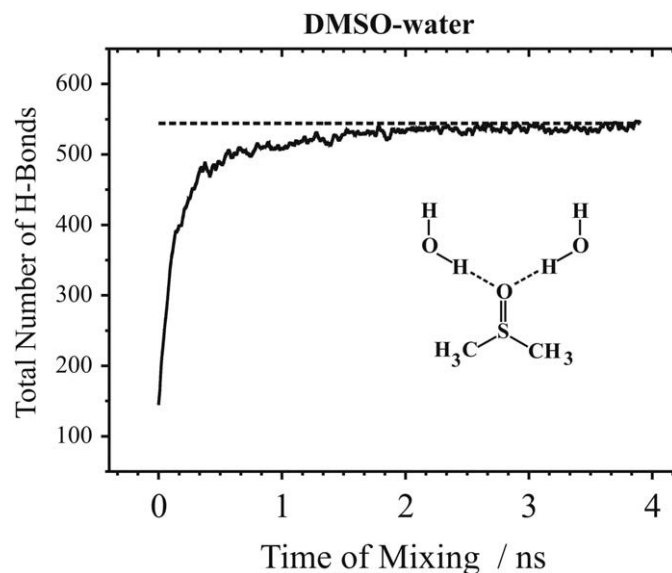


Fig. 3. The total number of H-bonds between DMSO and water as a function of the mixing time (in nanoseconds). A dotted line shows the maximal possible number of H-bonds for the studied DMSO/water system.

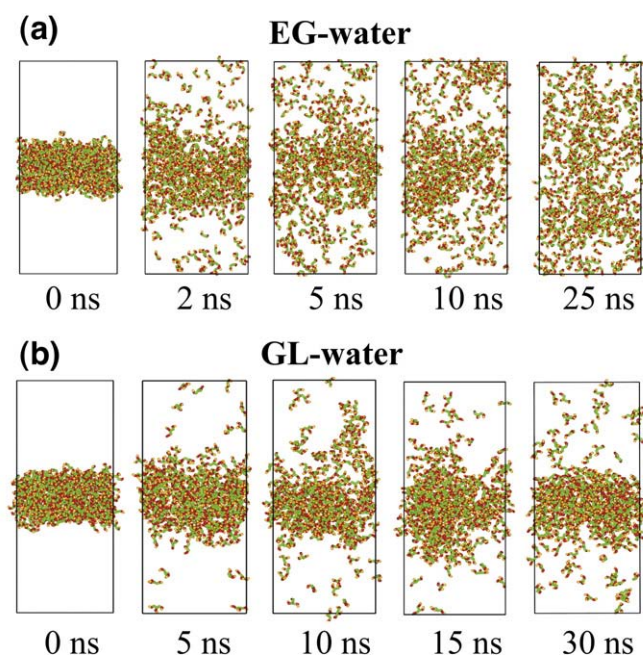


Fig. 4. Snapshots of the simulated boxes showing the distribution of CP solvent molecules in the binary EG/water (a) and GL/water (b) systems at the different mixing time periods. To clarify the presentation, the water molecules aren't shown.

clarity. As seen from Figs. 2(c) and 4(b), the mixing behavior in the GL/water system contrasts with what was observed in the two previous binary systems. The MD simulations, carried out in the same NPT conditions, reveal that in the case of the GL/water system the two phases mix with each other very slowly. As seen in Fig. 2(c), the mass density distributions display the clear phase separation within the system during the first mixing periods of 5–10 ns. The interface between the bulk-like GL phase and aqueous solution may be observed even at $t_m=15$ ns. The very slow phase mixing is also observed on the molecular level, Fig. 4(b).

The mixing behavior in the EG/water and GL/water systems on the molecular level is also considered in terms of the time evolution of hydrogen-bonding. In addition to hydrogen-bonding between CP and water molecules, H-bonding interactions acting between all CP molecules are also analyzed as a function of the mixing time. Fig. 5 shows a rapid increase in the number of hydrogen-bonds formed between all molecules of EG (blue) or GL (green) and water in the corresponding CP/water binary systems. Concurrently, at the same time the number of hydrogen-bonds between CP molecules decreases in an almost opposite fashion. A careful examination of the time evolution of hydrogen-bonding between EG and water allowed us to reveal two, fast and slow, time dependences. The rapid increase in the number of the H-bonds between EG and water, which is observed in Fig. 5 during first 5 ns, is followed by a very slow asymptotical dependence after $t_m>5$ ns. The increase in the number of EG–water H-bonds and the corresponding decrease in the number of the EG–EG H-bonds could be fitted by a two-exponential dependence, so that the fast component is found to be 1 ns and the slow component is extrapolated to be 50 ns, Fig. 5. The rapid decrease in the number of EG–EG H-bonds shows that, during the first mixing period, a spanning H-bond network within the bulk-like EG phase becomes partially broken. It seems that this disruption of the H-bond structure occurs due to some penetration of water molecules inside the bulk EG phase. As a result of breaking of the hydrogen-bond pattern, the bulk EG phase may be depleted into some aggregates of smaller sizes. This depletion is seen as the second slow component in the decay of the hydrogen-bonds number in Fig. 5. After the initial mixing stage, the EG aggregates are being transported into bulk water due to the thermal

diffusion. The mixing behavior in the GL/water system seems to be similar in many aspects to that of EG/water; however, due to the more complex three-dimensional H-bond network of the bulk GL solvent, the interphase mixing in GL/water occurs at a longer time scale. The two-exponential analysis of the increase of the number of the GL–water H-bonds reveals the fast component to be 5 ns. The fast component observed in the corresponding decrease of GL–GL hydrogen-bonding is estimated to be 3.5 ns, Fig. 5. The slow component could be extrapolated to 1–5 μ s with the same fitting quality. A further analysis allows us to conclude that in the EG/water and GL/water systems the mixing is controlled mainly by a rate of desorption of CP molecules from the bulk CP phase. The mixing timescale is found to be dependent on the structural organization and strength of the H-bond network formed between CP solvent molecules. It is, therefore, expected that the complete equilibration of the whole system in the three studied CP/water mixtures is occurring at significantly different timescales. Our MD study shows that the DMSO phase mix rapidly with bulk water during a few nanoseconds. In contrast to the DMSO/water system, the equilibration time of about 50 ns is needed to solubilize completely the bulk EG in water. Moreover, an asymptotic approximation of the mixing dynamics in the GL/water system has shown that the complete equilibration in this binary mixture should occur in the time scale of the order of microseconds.

3.3. DPPC membrane structure

One of the most important structural parameter of a lipid membrane is the surface area per one lipid molecule. This parameter describes packing of lipids in the plane of a membrane. The surface area per lipid is commonly used to ensure that an adequate bilayer model and force field are employed in MD simulations. In the case of a DPPC bilayer in pure water at $T=323$ K, we have estimated the average value of the surface area per lipid to be 65 ± 1 Å². This value agrees with the experimental data for the DPPC bilayer in the liquid crystalline phase [50]. Our MD results for all major structural and dynamics properties of the pure DPPC membrane are also found to be fully consistent with previous MD studies for the same bilayer [50]. Our analysis of regular bilayer properties in the ternary systems containing the CP agents indicates that the effect of CP on the overall structure of the membrane is found to

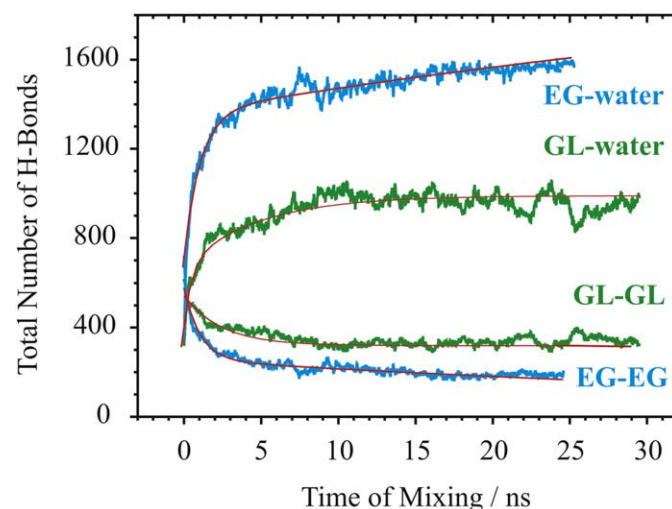


Fig. 5. Time evolution of hydrogen-bonding in EG/water and GL/water. The EG–water (blue) and GL–water (green) curves show the number of hydrogen-bonds between the CP solvents and water. The EG–EG (blue) and GL–GL (green) dependencies correspond to the total number of H-bonds between the CP molecules. Red curves show results of a two-exponential fitting (see Section 3.2 for details). (For interpretation of the references to color in this figure legend, the reader is referred to the web version of this article.)

be small. The area per lipid is slightly increased up to $67 \pm 1 \text{ \AA}^2$ in the CP/membrane/water ternary systems.

3.4. MD simulations of ternary CP/membrane/water systems

To gain insight into the mixing behavior and distribution of the CP solvents within the studied ternary systems, we first consider mass density profiles of different molecular components across the DPPC membrane.

Fig. 6(a) shows the mass density profiles of the individual components for the ternary DMSO/DPPC/water system calculated at $t_m=0$ ns. All the mass density profiles are plotted along the z-axis of the MD cell, so that the center of the z-axis corresponds to the lipid bilayer center. To compare the solubility dynamics of DMSO in pure water and in the aqueous/lipidic environment, a DMSO layer was placed nearly the membrane interface. As can be seen from Fig. 6(a), three mass density regions corresponding to the bulk aqueous solution, the DPPC bilayer, and DMSO can be identified in the DMSO/DPPC/water system. The solubility dynamics of the DMSO layer in aqueous solution is simulated by applying the MD conditions which are similar to those used in the previous simulations of the binary CP/water system. Interactions between DMSO and lipid molecules, as well as the favorable location of DMSO molecules within a hydrated DPPC bilayer, have already been computationally

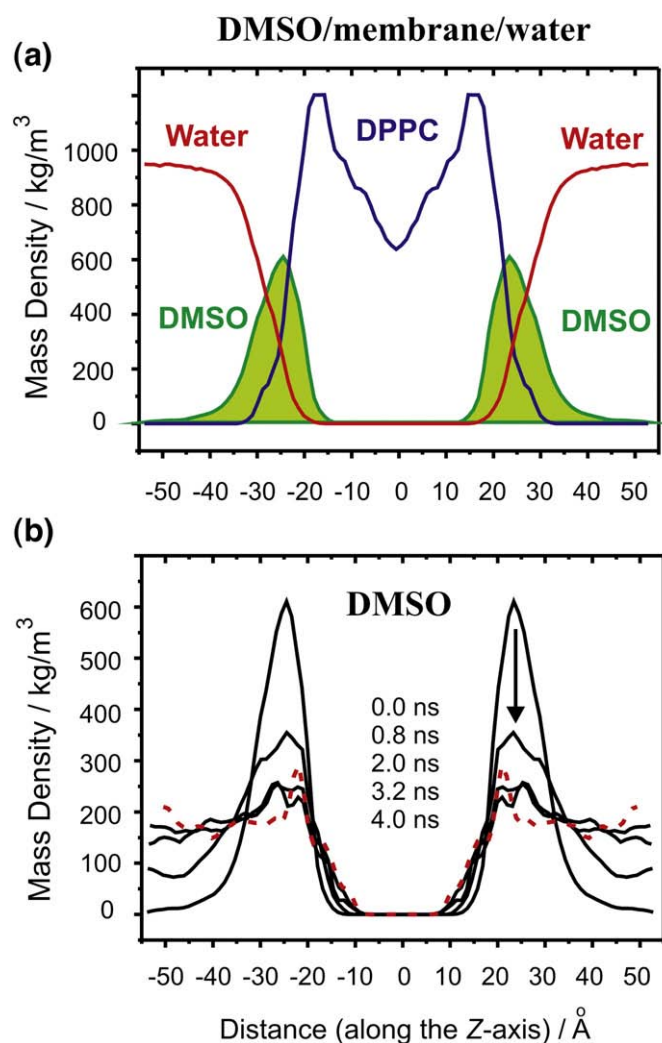


Fig. 6. Mass density profiles for individual components in the DMSO/membrane/water system at $t_m=0$ ns (a). DMSO mass density is calculated at different mixing periods (b). All the density profiles are plotted with respect to the center of the z-axis of the MD cell.

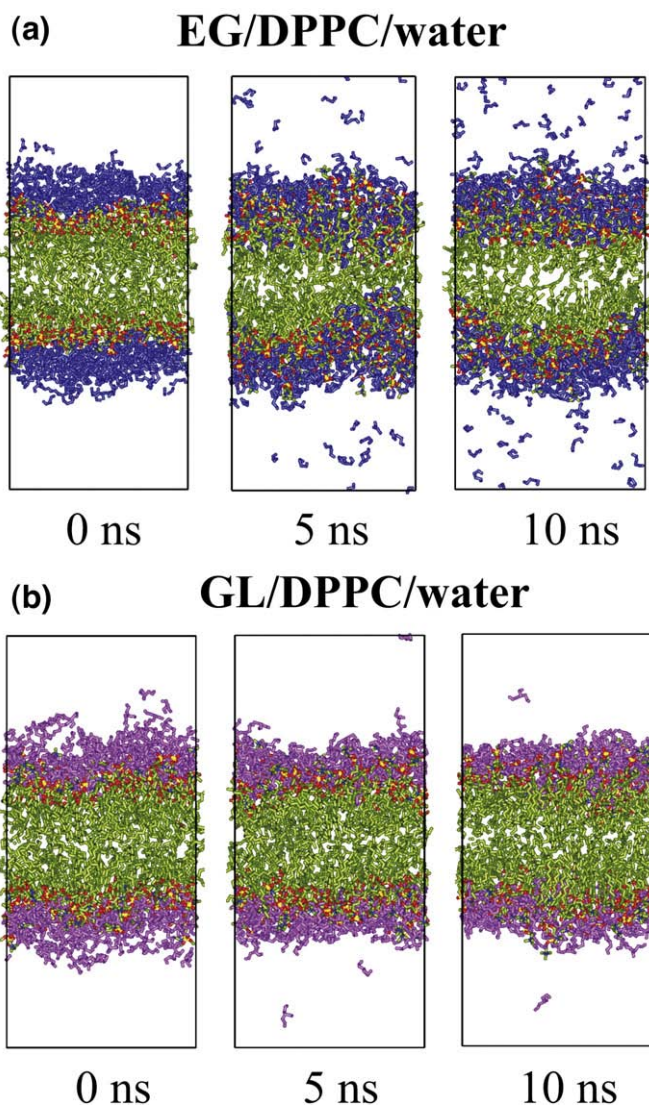


Fig. 7. Snapshots of the MD simulated boxes showing the distribution of the CP solvent molecules in the ternary EG/membrane/water (a) and GL/membrane/water (b) systems at the different times. EG and GL molecules are shown in blue (a) and magenta (b), respectively. To clarify the presentation, the water molecules aren't shown. (For interpretation of the references to color in this figure legend, the reader is referred to the web version of this article.)

studied by Sum and de Pablo at different DMSO contents [30]. Therefore, we mainly focus our analysis on an equilibration time and on the mixing dynamics of the DMSO component in the ternary system. The MD simulations show that the DMSO molecules mix rapidly with bulk water, so that during the first 2 ns a significant fraction of DMSO is tend to diffuse from the interfacial region into the aqueous solution. The dynamics of this diffusion is analyzed using the mass density distribution of the DMSO component at different simulation periods as shown in Fig. 6(b). A further analysis of energetic and dynamic parameters of the ternary DMSO/membrane/water system indicates that the system reaches the equilibrium state after approximately 4–5 ns of the MD simulation. This equilibrium state is characterized by uniform distribution of all DMSO molecules in the aqueous phase. It should also be noted that a peak of the DMSO mass density is observed at the distance of $\sim 20 \text{ \AA}$ from the bilayer center, as can be seen in Fig. 6(b) at $t_m=4$ ns. This feature can be understood in terms of some preferable binding of DMSO molecules to the membrane interface. The preferable binding of DMSO to the membrane surface has been experimentally suggested for the ternary

DMSO/DPPC/water systems [51–54]. In addition, the favorable location of DMSO at the interface has also been proposed by recent MD studies [30,31].

The mixing behavior of EG and GL is also studied for the corresponding ternary systems in the presence of the lipid membrane surrounded by bulk water. In these systems, CP molecules were also originally condensed as a thin layer between the DPPC membrane and water near the interface region. As an example, the initial EG/membrane/water system is shown in Fig. 1(bottom). Applying the same MD methodology, we simulate the partitioning behavior of EG and GL molecules between the lipidic and water environments. Fig. 7 (a–b) shows the time evolution of the distribution of EG and GL in the corresponding ternary systems at different periods of time. To improve the snapshot presentation the water molecules are not shown. As can be seen from Fig. 7, during the first equilibration periods the major population of the EG and GL molecules prefer to accumulate on the membrane surface, so that only a small fraction of the cryoprotector partitioned in the aqueous solution. The further analysis reveals that the EG and GL molecules interact strongly with zwitterionic phospholipid headgroups and, therefore, exhibits higher probability to reside at the DPPC interface.

Fig. 8 shows the time evolution of H-bonding between different molecular components in the ternary CP/DPPC/water systems. Similarly to the binary CP/water systems, we first consider H-bonding between CP–water and CP–CP. H-bonding interactions between all CP molecules and the DPPC membrane are also analyzed. In addition, H-bonding of CP with the DPPC membrane is considered separately for two functional groups of phospholipids which are able to form H-bonds; namely, for a choline group and carbonyl fragments of a glycerol moiety. Fig. 8 demonstrates that the total number of H-bonds between EG (or GL) molecules and water decreases gradually, Fig. 8(a–b). It is also seen that in the case of EG and GL, H-bonding between CP molecules itself is also decreased. At the same time, the number of H-bonds formed between CP and the DPPC membrane tends to increase. This result demonstrates that the EG and GL molecules favor the binding to the upper acyl chain and headgroup regions of the DPPC membrane. Our analysis of the interactions in the CP/DPPC/water systems shows that chemical nature of this binding is determined by a number of electrostatic interactions, including H-bonding to the phospholipid headgroup, and van-der-Waals CP–lipid interactions. The H-bonding between EG (or GL) and the membrane is mainly determined by H-bonding with oxygen atoms of the choline groups of the phospholipids as seen in Fig. 8(a–b).

Interestingly, the H-bonding analysis suggests that CP and water molecules compete with each other on the surface of the DPPC membrane. The basis for this competition is the capability of these compounds to form H-bonds with lipids. However, amphiphilic properties of the CP molecules give it more flexible capability to be attracted simultaneously to both hydrophobic and hydrophilic centers of the membrane surface. Therefore, CP agents with higher hydrophilic character, such as EG and GL, are able to bind to certain centers of the membrane surface preferentially. They displace water leading to some membrane dehydration.

The time evolution of the mixing dynamics of the CP components being in contact with the DPPC/water interface is analyzed using the mass density distribution and the H-bonding analysis. The comparison of the mixing dynamics in the binary and tertiary systems shows that the mixing timescale becomes much longer in the case of the ternary systems. We have analyzed the depletion dynamics of large EG and GL aggregates in the presence of the lipid membrane during 15–20 ns of the MD simulations. The simulations show dramatic slowing down of the depletion dynamics of the CP aggregates. The simulation time seems, however, to be not enough to ensure adequate MD sampling. These results suggest that the presence of the lipid membrane introduces the strong competition due to the intermolecular interactions between lipid and CP, and also between CP and water. Such a complex mixing behavior of large CP clusters occurring

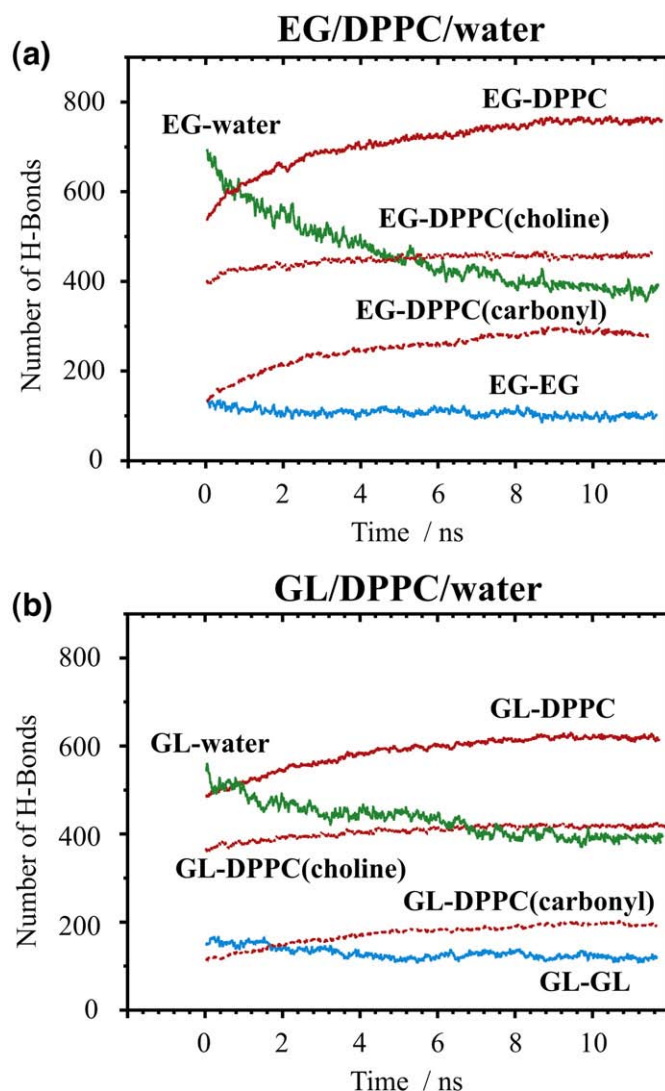


Fig. 8. Time evolution of hydrogen-bonding in the EG/DPPC/water (a) and GL/DPPC/water (b) systems. The EG–water and GL–water (green) curves show the number of H-bonds between the CP solvents and water. The EG–DPPC and GL–DPPC (red) curves correspond to the total number of H-bonds between all the CP molecules and DPPC. In the last case, the H-bonding contributions of the choline and carbonyl groups of the membrane are plotted separately. The EG–EG and GL–GL (blue) dependencies correspond to the total number of H-bonds formed between all the CP molecules. (For interpretation of the references to color in this figure legend, the reader is referred to the web version of this article.)

in contact with the aqueous/lipid environment may be some reason for large concentration gradients in cellular cryosolutions.

Based on our MD results it is interesting to note that many properties of organic CP agents, such as degree and energy of their self-association, structure and length of H-bond networks are of particular interest for cryoconservation since these parameters determine the temperature behavior of cryosolution during freezing. However, mixtures of water with organic solvents, which have several polar functional groups, have been much less studied than solutions of monofunctional CP agents [55]. Polyfunctional amphiphilic compounds such as diols and glycerols form a complex three-dimension network of H-bonds in aqueous solution [17]. Among these polyfunctional solutes, mixtures of ethylene glycol with water have been most studied in terms of their thermochemical and thermodynamical properties [56]. However, even for this system the microstructure of the mixed solvent composition is still not understood completely. Recent experimental data have provided evidences that interactions of CP agents with water are concentration-dependent [5–9,17–19,55]. In addition, the concentration dependence of physical

properties of CP–water mixtures is found to be non-linear. This nonlinearity is known for DMSO–water mixtures [57]. It has been noted that changes of physico-chemical parameters of the DMSO–water mixtures are characterized by maxima and minima at DMSO molar fraction $X_{\text{DMSO}}=0.3\pm0.4$ [58]. The microstructure of the DMSO–water mixtures has also been studied by neutron diffraction [59]. However, the influence of DMSO on the microstructure of water solution has not been discussed in details. It has only been observed that the number of water–water hydrogen-bonding in these mixtures is decreased compared to that of in pure water. Numerous experimental and theoretical studies have provided convenient evidences that aqueous solutions of organic components are characterized by the microheterogeneous structure. The microheterogeneity of the organic component in such solution is often accompanied by local concentration fluctuations. On the other hand, the structure, size and lifetime of these aggregates are still a subject of intensive investigations and discussions.

Since a lipid bilayer serves as a structural basis for cell membranes, it is often considered as a primary model for a molecular understanding of reversible action of small amphiphilic molecules on cellular solution. This is why it is important to know the mechanism that enables some organic solvents to be a very effective CP agent. Recently, distribution of alcohol molecules across a palmitoyl-oleoyl-phosphatidylcholine (POPC) bilayer has been studied by NMR experiments and MD simulations [60]. The results shown that ethanol interacts with a POPC membrane primarily via hydrophilic interactions, in particular due to the formation of hydrogen-bonds to the lipid phosphate group. A recent MD investigation has also supported these results and shows that short-chain alcohols exhibit some preference to occupy regions near the upper part of the lipid acyl chains and the phosphatidylcholine headgroups [33,34,61,62]. Additionally, it has been shown that, in a homologous series of aliphatic *n*-alcohols with an intermediate chain length, an increase in the number of carbon atoms of an alkyl chain (butanol, pentanol and hexanol) results in a gradual decrease in hydrophilic solute–membrane interactions, so that a partitioning process and packing of solute molecules in alcohol/membrane/water systems are driven mainly by hydrophobic forces [63,64].

4. Conclusions

The mixing behavior of the cryoprotective solvents (DMSO, ethylene glycol (EG), and glycerol (GL)) in aqueous and aqueous/lipidic environments is examined employing molecular dynamics (MD) methodology. We investigated the equilibration timescale which is required to mix a large CP cluster with water. This timescale is estimated by considering the depletion dynamics of the CP cluster in pure water and in solution at an aqueous/membrane interface. The MD analysis has demonstrated that the bulk DMSO phase mix rapidly with water, so that in the equilibrium aqueous solution all the DMSO molecules are uniformly distributed across the MD box. The simulations also confirm that, in the equilibrium aqueous solution, the DMSO molecules exist as an H-bonded complex in which one DMSO molecule is simultaneously bonded with two water molecules. Our investigation of the microstructure of the binary solutions containing EG and GL has revealed however that, despite the CP agents and water being fully miscible in all proportions, they are not ideally mixed at the molecular level. The EG and GL solvents, which are introduced as the large cluster into aqueous solution, tend to preserve their intrinsic structural order upon dilution. Our MD study shows that the mixing dynamics of between EG (or GL) and surrounding bulk water is found to be strongly dependent on nature of hydrophilic and hydrophobic interactions acting between cryoprotectant molecules. We have found that the intermolecular interactions play a decisive role in the mixing of these CP agents with water. The mixing in the EG/water and GL/water systems is, therefore, controlled mainly by the rate of desorption of individual CP molecules from the bulk-like CP cluster. The different amphiphilic nature of the studied CP solvents results in strong hydrophilic and hydrophobic intermolecular

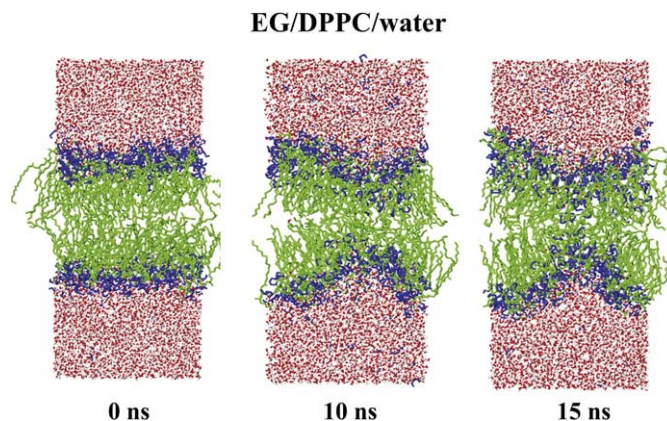


Fig. 9. Examples of membrane defects and damages induced by cryoprotector molecules in the EG/DPPC/water systems.

interactions acting between CP molecules. The depletion of their bulk-like CP structure is, therefore, occurring at significantly different timescales. Our MD study demonstrates that, in contrast to the DMSO/water system, the timescale of the depletion of the EG cluster in pure water is estimated to be in the order of 50 ns. The solubilization time of the bulk GL cluster in the surrounding water could not be determined directly, so that this value could be approximated asymptotically. The complete equilibration in this binary mixture is therefore expected to occur in the timescale of the order of microseconds.

The study indicates that the favorable binding of CP aggregates with the membrane surface results in dramatic slowing down the equilibration process in the aqueous/lipidic environment. Moreover, the high CP concentrations appearing during the long-term local contact of a CP cluster with a membrane surface may be a reason for some disturbance of the lipid packing and the formation of membrane defects. As a result, such fluctuations of the local concentration of CP are able to induce the irreversible damage of cell membranes, which is expected to be the reason for the cytotoxic effect of cryoprotectant [66]. Such deformations and damages of the DPPC membrane have indeed been observed for some of our MD runs as shown in Fig. 9. Further investigation of this phenomenon will include concentration dependence of cryoprotector-induced damages of lipid membranes and such simulations are planned for further studies. Recent MD simulations have also suggested that small amphiphilic molecules, such as DMSO, may induce the local loss in integrity of the bilayer structure [31,65]. The current finding of the long-term microheterogeneity in cryosolutions can stimulate further studies on identifying an optimal practical application of CP agents in cryobiology and cryomedicine.

References

- [1] P. Mazur, C. Koshimoto, Is intracellular ice formation the cause of death of mouse sperm frozen at high cooling rate? *Biol. Reprod.* 66 (2002) 1485–1490.
- [2] K.R. Harris, P.J. Newitt, Diffusion and structure in dilute aqueous alcohol solutions: evidence for the effects of large apolar solutes on water, *J. Phys. Chem. B* 102 (1998) 8874–8879.
- [3] S. Dixit, J. Crain, W.C.K. Poon, J.L. Finney, A.K. Soper, Molecular segregation observed in a concentrated alcohol–water solution, *Nature* 416 (2002) 829–832.
- [4] M. D' Angelo, G. Onori, A. Santucci, Self-association of monohydric alcohols in water: compressibility and infrared absorption measurements, *J. Chem. Phys.* 100 (1994) 3107–3113.
- [5] N. Nishi, S. Takahashi, M. Matsumoto, A. Tanaka, K. Muraya, T. Takamuku, T. Yamaguchi, Hydrogen bonding cluster formation and hydrophobic solute association in aqueous solution of ethanol, *J. Phys. Chem.* 99 (1995) 462–468.
- [6] A. Wakisaka, H. Abdoul-Carime, Y. Yamamoto, Y. Kiyozumi, Non-ideality of binary mixtures. Water–methanol and water–acetonitrile from the viewpoint of clustering structure, *J. Chem. Soc. Faraday Trans.* 94 (1998) 369–374.
- [7] K. Egashira, N. Nishi, Low-frequency Raman spectroscopy of ethanol–water binary solution: evidence for self-association of solute and solvent molecules, *J. Phys. Chem. B* 102 (1998) 4054–4057.
- [8] S.S.N. Murthy, Detailed study of ice clathrate relaxation: evidence for the existence of clathrate structures in some water–alcohol mixtures, *J. Phys. Chem. A* 103 (1999) 7927–7937.

- [9] A. Wakisaka, S. Komatsu, Y. Usui, Solute–solvent and solvent–solvent interactions evaluated through clusters isolated from solutions: preferential solvation in water–alcohol mixtures, *J. Mol. Liq.* 90 (2001) 175–184.
- [10] D.T. Bowron, J.L. Finney, A.K. Soper, Structural investigation of solute–solute interactions in aqueous solutions of tertiary butanol, *J. Phys. Chem. B* 102 (1998) 3551–3563.
- [11] L. Dougan, S.P. Bates, R. Hargreaves, J.P. Fox, J. Crain, J.L. Finney, V. Réat, A.K. Soper, Methanol–water solutions: a bi-percolating liquid mixture, *J. Chem. Phys.* 121 (2004) 6456–6462.
- [12] T. Takamuku, H. Maruyama, K. Watanabe, T. Yamaguchi, Structure of 1-propanol–water mixtures investigated by large-angle X-ray scattering technique, *J. Solution Chem.* 33 (2004) 641–660.
- [13] I.I. Vaisman, M.L. Berkowitz, Local structural order and molecular associations in water–DMSO mixtures. Molecular dynamics study, *J. Am. Chem. Soc.* 114 (1992) 7889–7896.
- [14] A. Luzar, D. Chandler, Structure and hydrogen bond dynamics of water–dimethyl sulfoxide mixtures by computer simulations, *J. Chem. Phys.* 98 (1993) 8160–8173.
- [15] A. Vishnyakov, A.P. Lyubartsev, A. Laaksonen, Molecular dynamics simulations of dimethyl sulfoxide and dimethyl sulfoxide–water mixture, *J. Phys. Chem. A* 105 (2001) 1702–1710.
- [16] P. Bordat, A. Lebrét, J.P. Demaret, F. Affouard, M. Descamps, Comparative study of trehalose, sucrose and maltose in water solutions by molecular modeling, *Europhys. Lett.* 65 (2004) 41–47.
- [17] J.L. Dashnau, N.V. Nucci, K.A. Sharp, J.M. Vanderkooi, Hydrogen bonding and the cryoprotective properties of glycerol/water mixtures, *J. Phys. Chem. B* 110 (2006) 13670–13677.
- [18] D.T. Bowron, A.K. Soper, J.L. Finney, Temperature dependence of the structure of a 0.06 mole fraction tertiary butanol–water solution, *J. Chem. Phys.* 114 (2001) 6203–6219.
- [19] L. Dougan, R. Hargreaves, S.P. Bates, J.L. Finney, V. Réat, A.K. Soper, J. Crain, Segregation in aqueous methanol enhanced by cooling and compression, *J. Chem. Phys.* 122 (2005) 174514–174517.
- [20] G.J. Morris, M. Goodrich, E. Acton, F. Fonseca, The high viscosity encountered during freezing in glycerol solutions: effects on cryopreservation, *Cryobiology* 52 (2006) 323–334.
- [21] C.J. Hunt, D.E. Pegg, S.E. Armitage, Optimizing cryopreservation protocols for haematopoietic progenitor cells: a methodological approach for umbilical cord blood, *CryoLetters* 27 (2006) 73–86.
- [22] N. Takanashi, Effect of cryoprotectants on the viability and functions of unfrozen human polymorphonuclear cell, *Cryobiology* 20 (1985) 336–350.
- [23] M.J. Taylor, C.J. Hunt, Tolerance of corneas to multimolar dimethyl sulfoxide at 0 degrees C. Implications for cryoconservation, *Invest. Ophthalmol. Vis. Sci.* 30 (1989) 400–412.
- [24] A.R. Silva, R.C. Cardoso, D.C. Uchoa, L.D. Silva, Quality of canine semen submitted to single or fractionated glycerol addition during the freezing process, *Theriogenology* 59 (2003) 821–829.
- [25] F. Penninckx, N. Cheng, R. Kerremans, B. van Damme, W. de Loecker, The effects of different concentrations of glycerol and dimethylsulfoxide on the metabolic activities of kidney slices, *Cryobiology* 20 (1983) 51–60.
- [26] R. McClean, C. MacCallum, D. Blyde, W.V. Holt, S.D. Johnson, Ultrastructure, osmotic tolerance, glycerol toxicity and cryopreservation of caput and cauda epididymal kangaroo spermatozoa, *Reprod. Fertil. Dev.* 18 (2006) 469–476.
- [27] S. He, L.C. Woods, Effects of dimethyl sulfoxide and glycine on cryopreservation induced damage of plasma membranes and mitochondria to striped bass (*Morone saxatilis*) sperm, *Cryobiology* 48 (2004) 254–262.
- [28] S. Adler, C. Pellizer, M. Paparella, T. Hartung, S. Bremer, The effects of solvents on embryonic stem cell differentiation, *Toxicol. In Vitro* 20 (2006) 265–271.
- [29] T.J. Anchordoguy, J.F. Carpenter, J.H. Crowe, L.M. Crowe, Temperature-dependent perturbation of phospholipid bilayers by dimethylsulfoxide, *Biochim. Biophys. Acta* 1104 (1992) 117–122.
- [30] A.K. Sum, J.J. de Pablo, Molecular simulation study on the influence of dimethylsulfoxide on the structure of phospholipid bilayers, *Biophys. J.* 85 (2003) 3636–3645.
- [31] R. Notman, M. Noro, B. O. 'Malley, J. Anwar, Molecular basis for dimethylsulfoxide (DMSO) action on lipid membranes, *J. Am. Chem. Soc.* 128 (2006) 13982–13983.
- [32] M.A. Villarreal, S.B. Díaz, E.A. Disalvo, G.G. Montich, Molecular dynamics simulation study of the interaction of trehalose with lipid membranes, *Langmuir* 20 (2004) 7844–7851.
- [33] A.N. Dickey, R. Faller, Investigating interactions of biomembranes and alcohols: a multiscale approach, *J. Polym. Sci. B* 43 (2005) 1025–1032.
- [34] J. Chanda, S. Bandyopadhyaya, Perturbation of phospholipid bilayer properties by ethanol at a high concentration, *Langmuir* 22 (2006) 3775–3781.
- [35] J. Chanda, S. Chakraborty, S. Bandyopadhyay, Sensitivity of hydrogen bond lifetime dynamics to the presence of ethanol at the interface of a phospholipid bilayer, *J. Phys. Chem. B* 110 (2006) 3791–3797.
- [36] S. Leekumjorn, A.K. Sum, Molecular study of the diffusional process of DMSO in double lipid bilayers, *Biochim. Biophys. Acta* 1758 (2006) 1751–1758.
- [37] E. Lindahl, B. Hess, D. van der Spoel, GROMACS 3.0: a Package for molecular simulation and trajectory analysis, *J. Mol. Model.* 7 (2001) 306–317.
- [38] H. Liu, F. Müller-Plathe, W.F. van Gunsteren, A force field for liquid dimethyl sulfoxide and physical properties of liquid dimethyl sulfoxide calculated using molecular dynamics simulation, *J. Am. Chem. Soc.* 117 (1995) 4363–4366.
- [39] H. Hayashi, H. Tanaka, K. Nakanishi, Molecular dynamics simulations of flexible molecules. Part I. Aqueous solution of ethylene glycol, *J. Chem. Soc. Faraday Trans.* 91 (1995) 31–39.
- [40] L. Saiz, J.A. Padró, E. Guàrdia, Structure of liquid ethylene glycol: a molecular dynamics simulation study with different force fields, *J. Chem. Phys.* 114 (2001) 3187–3199.
- [41] A.V. Gubskaya, P.G. Kuslik, Molecular dynamics simulation study of ethylene glycol, ethylenediamine, and 2-aminoethanol. 1. The local structure in pure liquids, *J. Phys. Chem. A* 108 (2004) 7151–7164.
- [42] R. Chelli, P. Procacci, G. Cardini, R.G.D. Valle, S. Califano, Glycerol condensed phases. Part I. A molecular dynamics study, *Phys. Chem. Chem. Phys.* 1 (1999) 871–877.
- [43] R. Chelli, P. Procacci, G. Cardini, S. Califano, Glycerol condensed phases. Part II. A molecular dynamics study of the conformational structure and hydrogen bonding, *Phys. Chem. Chem. Phys.* 1 (1999) 879–885.
- [44] J. Bleick, F. Affouard, P. Bordat, A. Lebrét, M. Descamps, Molecular dynamics simulations of glycerol glass-forming liquid, *Chem. Phys.* 317 (2005) 253–257.
- [45] D.P. Tieleman, H.J.C. Berendsen, Molecular dynamics simulations of a fully hydrated dipalmitoylphosphatidylcholine bilayer with different macroscopic boundary conditions and parameters, *J. Chem. Phys.* 105 (1996) 4871–4880.
- [46] J. Hermans, H.J.C. Berendsen, W.F. van Gunsteren, J.P.M. Postma, A consistent empirical potential for water–protein interactions, *Biopolymers* 23 (1984) 1513–1518.
- [47] H.J.C. Berendsen, J.P.M. Postma, W.F. van Gunsteren, A. DiNola, J.R. Haak, Molecular dynamics with coupling to an external bath, *J. Chem. Phys.* 81 (1984) 3684–3690.
- [48] T. Darden, D. York, L. Pedersen, Particle mesh Ewald: an N-log(N) method for Ewald sums in large systems, *J. Chem. Phys.* 98 (1993) 10089–10092.
- [49] B. Hees, H. Bekker, H.J.C. Berendsen, J.G.E.M. Fraaije, LINCS: a linear constraint solver for molecular simulations, *J. Comput. Chem.* 18 (1997) 1463–1472.
- [50] C. Anézo, A.H. de Vries, H.D. Höltje, D.P. Tieleman, S.J. Marrink, Methodological issues in lipid bilayer simulations, *J. Phys. Chem. B* 107 (2003) 9424–9433.
- [51] V.I. Gordeliy, M.A. Kiselev, P. Lesieur, A.V. Pole, J. Teixeira, Lipid membrane structure and interactions in dimethyl sulfoxide/water mixtures, *Biophys. J.* 75 (1998) 2343–2351.
- [52] M.A. Kiselev, P. Lesieur, A.M. Kiselev, M. Ollivon, Ice formation in model biological membranes in the presence of cryoprotectors, *Nucl. Instrum. Methods Phys. Res. A* 448 (2000) 255–260.
- [53] H.H. Chang, P.K. Dea, Insights into the dynamics of DMSO in phosphatidylcholine bilayers, *Biophys. Chem.* 94 (2001) 33–40.
- [54] M.A. Kiselev, T. Gutberlet, P. Lesieur, T. Hauss, M. Ollivon, R.H.H. Neubert, Properties of ternary phospholipid/dimethyl sulfoxide/water systems at low temperatures, *Chem. Phys. Lipids* 133 (2005) 181–193.
- [55] D.V. Batov, A.M. Zaichikov, V.P. Slyusar, V.P. Korolev, Enthalpies of mixing and state of components in aqueous–organic mixtures with nets of hydrogen bonds, *Russ. J. Gen. Chem.* 71 (2001) 1208–1214.
- [56] J.-Y. Huot, E. Battistel, R. Lumry, G. Villeneuve, J.-F. Lavalley, A. Anusiem, C. Jolicoeur, A comprehensive thermodynamic investigation of water–ethylene glycol mixtures at 5, 25, and 45 °C, *J. Solution Chem.* 17 (1988) 601–636.
- [57] E. Tommila, A. Pajunen, The dielectric constants and surface tensions of dimethyl sulfoxide–water mixtures, *Suom. Kemistilehti. B* 41 (1969) 172–176.
- [58] E.A. Guggenheim, *Mixtures*, Clarendon Press, Oxford, 1952.
- [59] A.K. Soper, A. Luzar, A neutron diffraction study of dimethyl sulfoxide–water mixtures, *J. Chem. Phys.* 37 (1992) 1320–1331.
- [60] S.E. Feller, C.A. Brown, D.T. Nizza, K. Gawrisch, Nuclear Overhauser enhancement spectroscopy cross-relaxation rates and ethanol distribution across membranes, *Biophys. J.* 82 (2002) 1396–1404.
- [61] B.W. Lee, R. Faller, A.K. Sum, I. Vattulainen, M. Patra, M. Karttunen, Structural effects of small molecules on phospholipid bilayers investigated by molecular simulations, *Fluid Phase Equilib.* 225 (2004) 63–68.
- [62] M. Patra, E. Salonen, E. Terama, I. Vattulainen, R. Faller, B.W. Lee, J. Holopainen, M. Karttunen, Under the influence of alcohol: the effect of ethanol and methanol on lipid bilayers, *Biophys. J.* 90 (2006) 1121–1135.
- [63] P. Westh, C. Trandum, Partitioning of small alcohols into dimyristoyl phosphatidylcholine (DMPC) membranes: volumetric properties, *J. Phys. Chem. B* 104 (2000) 11334–11341.
- [64] U.R. Pedersen, G.H. Peters, P. Westh, Molecular packing in 1-hexanol-DMPC bilayers studied by molecular dynamics simulation, *Biophys. Chem.* 125 (2007) 104–111.
- [65] A.A. Gurtovenko, J. Anwar, Modulating the structure and properties of cell membranes: the molecular mechanism of action of dimethyl sulfoxide, *J. Phys. Chem. B* 111 (2007) 10453–10460.
- [66] G.M. Fany, T.H. Lilley, H. Linsdell, M.S. John, H.T. Meryman, Cryoprotectant toxicity and cryoprotectant toxicity reduction: in search of molecular mechanisms, *Cryobiology* 27 (1990) 247–268.